Supplementary Materials

Crossed stretchable zipper

Fanming Wang[1,2], Chun Feng[3], Zhitong Wang[4], Yewang Su[1,2,*]

[1]State Key Laboratory of Nonlinear Mechanics, Institute of Mechanics, Chinese Academy of Sciences, Beijing 100190, China.
[2]School of Engineering Science, University of Chinese Academy of Sciences, Beijing 100049, China.
[3]Key Laboratory for Mechanics in Fluid Solid Coupling Systems, Institute of Mechanics, Chinese Academy of Sciences, Beijing 100190, China.
[4]Wide Range Flight Engineering Science and Applications Center, Institute of Mechanics, Chinese Academy of Sciences, Beijing 100190, China.

[*]**Correspondence to:** Prof. Yewang Su, State Key Laboratory of Nonlinear Mechanics, Institute of Mechanics, Chinese Academy of Sciences, Beijing 100190, China. E-mail: yewangsu@imech.ac.cn

MAIN TEXT

Supplementary Text 1. Calculation of the critical strain for dividing different initial contact conditions.

The inner sidewalls of the novel slider feature symmetrically arranged movable blocks equipped with springs, which flexibly move along the grooves under pressure. This design ensures normal interlocking and separation of the teeth under different strain conditions. However, the movable blocks' unexpected motion may cause interlocking failure or jamming of the sub-parts within the slider. As shown in Figure 1E and 1F, a fixed inner sidewall is added at the upper edge of the movable blocks to minimize redundant rotational movement of sub-parts, effectively stabilizing them under minor external disturbances or low slider extrusion forces. Nevertheless, tolerances in the slider's internal space and increased compressive forces during interlocking can still induce redundant rotation if the cross adapter's structure is suboptimal, potentially leading to interlocking failure. To address this, the conditions under which sub-parts may rotate during interlocking are systematically studied, as shown in Figure S7. When the two side sub-parts first contact within the slider, the distance between their bottom corners is calculated as

$$H_{corner}=2\left(L_{s\text{-}p}\text{-}R\right)\cos\ \theta+\sqrt{(2R)^2\text{-}D_{corner}^2} \tag{S1}$$

where H_{corner} is the distance between the bottom corners of the A_1 and B_1, L_{s-p} is the length and width of the sub-parts, $R=2.4\text{mm}$ is the radius of the arc at the front end of both the slot's sidewalls and the latch, $\theta=10^{\circ}$ is the angle between the track and the symmetry plane, and $D_{corner}=2.4\text{mm}$ is the horizontal distance between the centers of the arcs at the front ends of the latch and the slot. Equation (S1) shows that, for the given parameters, the contact initiation position of the sub-parts remains unchanged during both unilateral and bilateral interlocking. To prevent interlocking failure due to rotational motion, the sub-part system must satisfy

$$\begin{cases} [(p_1\text{-}p_2)l+(P_3\text{-}P_4)](\cos\theta\text{-}\mu\sin\theta)=0 \\ \dfrac{1}{2}H_1\cos\theta\begin{bmatrix}(p_1\text{-}p_2)l+\\ \mu(P_3\text{-}P_4)\end{bmatrix}\text{-}\begin{Bmatrix}\left[\dfrac{1}{2}\left(L_{s\text{-}p}+l\right)\text{-}l_1\right]P_4\ \text{-}\\ \left[\dfrac{1}{2}\left(W_{s\text{-}p}+l\right)\text{-}l_1\right]P_3\text{-}FL\end{Bmatrix}=\dfrac{1}{2}(2ll_1\text{-}l^2)(p_1\text{-}p_2) \end{cases} \tag{S2}$$

where p_1 is the normal pressure exerted by the slider on A_1, p_2 represents the normal pressure exerted by the slider on B_1, l is the distance along the track direction

between the bottom corners of A_1, B_1 and the edge of the movable abdication block, P_3 is the normal pressure exerted by M_1 on A_1, P_4 is the normal pressure exerted by M_2 on B_1, μ is the dynamic friction coefficient between the components within the slider, $H_1 = H_{corner} + 6.4\sin\theta(1+\tan\theta)$ is the distance between the inner sidewalls of the slider along the line connecting the centroid of A_1 (C_{A1}) and the centroid of B_1 (C_{B1}), $W_{s-p} = 0.625L_{s-p}$ is the width of the suture-joint structure of A_1 and B_1, l_1 is the distance along the track direction between the centroid of the sub-part system (C_{AB}) and the bottom corner of the sub-parts, F is the resultant force of the elastic band on the sub- part system, and L is the distance from the centroid of the sub- parts system to the point where the resultant force acts.

By analyzing Equation (S2) and Supplementary Figure S7, a simple and effective method to prevent rotation of the sub-part system is to reduce the length L_{s-p} of the sub-parts. This adjustment shifts the contact position of the sub-parts within the slider closer to the exit. Consequently, when L_{s-p} is reduced below a specific threshold, the moment generated by the normal pressure of the slider inner sidewall on the sub-parts' centroid becomes zero. Under this condition, the second equation in Equation (S2) can be expressed as:

$$\frac{1}{2}\left[D_{blocks}-\frac{1}{2\sin\theta}(H_{corner}-H_{tw})\right]=3.2(1+\tan\theta)-\frac{1}{2}H_1\sin\theta \qquad (S3)$$

where $D_{blocks} = 12\text{mm}$ is the distance along the track direction between the turning point of the track and the edge of the movable abdication block, $H_{tw} = 14\text{mm}$ is the width of the slider track after convergence. Solving Equation (S3) shows that when $L_{s-p} \le 8.7\text{mm}$, the sub-parts do not undergo rotational motion during the interlocking process within the slider.

Supplementary Text 2. Anti-interference performance of the crossed stretchable zipper in the toothless overlapping area.

In the crossed stretchable zipper system, the slider width is 32.39 mm. To ensure normal zipping and unzipping, a tooth-free zone must be established near the overlapping part of the zipper (Supplementary Figure S8). Based on repeated zipping and unzipping tests, the length of this zone is reasonably set at 1.5-1.6 times the slider width. Within this zone, the effective interlocking ratio can be given as

$$r_{effective} = \frac{W_{c\text{-}a}}{1.6W_{slider}} \tag{S4}$$

where $r_{effective}$ is the ratio of the true interlocking length to the total length of the area, W_{c-a} is the side length of the cross adapter, and W_{slider} is the width of the slider.

The breaking force and anti-separation force in the toothless overlapping area under different effective interlocking ratios are summarized in Supplementary Table 1.

Supplementary Table 1. The breaking force and anti-separation force at the toothless overlapping area under different effective interlocking ratios

	$r_{effective}$ (%)	Breaking force (N)	Anti-separation force (N)
Toothless overlapping area	27	10.2	15.6
	26	9.5	15.3
	25	9.1	14.8
	24	8.5	14.7
	23	7.8	14.3

The breaking force and anti-separation force of interlocked teeth under different strain conditions, with no strain difference between the two tapes, are presented in Supplementary Table 2.

Supplementary Table 2. The breaking force and anti-separation force of interlocked teeth under different strain conditions

	Strain Value (%)	Breaking force (N)	Anti-separation force (N)
Interlocked teeth	0	8.8	10.6
	5	8.1	10.2
	10	6.6	9.5
	15	6.0	8.9
	20	4.9	8.6
	25	4.3	7.6

To ensure sufficient anti-interference performance, the effective interlocking ratio of the toothless overlapping area must be at least 25%. At this ratio, the breaking force of the overlapping area is comparable to that of the interlocked teeth, while its separation resistance is higher, meeting the performance requirements of the crossed stretchable zipper. Based on the above analysis, $r_{effective} = 25\%$ and $W_{c-a} = 13\text{mm}$. Considering the overlapping length of the sub-parts at the suture-joint structure, then for the sub-part, $L_{s-p} = 8\text{mm}$ and $W_{s-p} = 6\text{mm}$. This configuration prevents unexpected rotation of the sub-parts during interlocking while allowing the overlapping area to maintain excellent anti-interference performance.

Supplementary Text 3. The expected practical application scenarios of the three typical scenarios.

The partial interlock state occurs when each pair of the four sub-parts of the cross adapter achieves one-sided locking, forming two non-interlocking structures. This typically arises when one set of zippers connects two functional fabrics (with specific functions), while the other set acts as open-type functional zippers for easy wearing, removal, or access. In such cases, if one functional fabric needs adjustment or replacement without closing the open-type zippers, the cross adapter transitions from full separation to partial interlock. Notably, the zippers connecting the two functional fabrics usually experience zero strain, as the unclosed open-type zippers act as free boundaries, whereas the strain of the open-type zippers can vary depending on actual conditions.

The full interlock under symmetric stretching occurs when all four sub-parts of the cross adapter achieve two-sided locking, with the strains of the tapes on both sides of the stretchable zipper being equal. This is the most common scenario for crossed stretchable zippers, typically when connecting four sets of functional fabrics. In such cases, if the stretchable zippers in one direction function as openings for easy wearing, removal, or access, frequent zipping/unzipping along that direction is required. Similarly, the adjustment or replacement of two functional fabrics involves opening and closing along a specific direction. During these processes, the cross adapter transitions from partial interlock to full interlock under symmetric stretching, and the crossed stretchable zippers may experience varying degrees of strain in both directions.

The full interlock state under asymmetric stretching occurs when all four sub-parts of the cross adapter achieve two-sided locking, with the strains of the tapes on both sides of the stretchable zipper being unequal. This state is generally a variant of the full interlock under symmetric stretching and is typically used to fully interconnect four sets of functional fabrics. The unequal strains may arise actively, due to specific usage requirements, or passively, from uneven tensile forces. For example, to conform to a curved edge, the crossed stretchable zippers must be arranged along that edge, resulting in unequal tape strains. Similarly, uneven loading can cause the two tapes to experience different tensile forces, producing unequal strains.

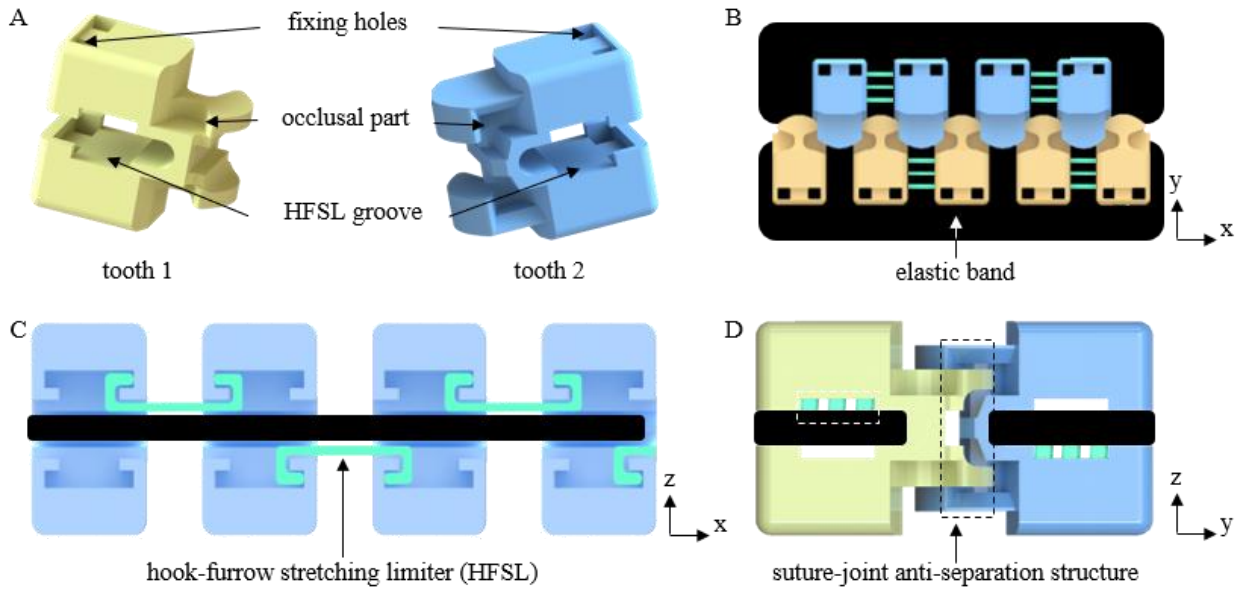

Supplementary Figure 1. The specific structure of the stretchable zipper. (A) The specific structure of the chain teeth; (B) Spatulate interlocking structure; (C) Over-stretching restriction structure; (D) Anti-separation structure.

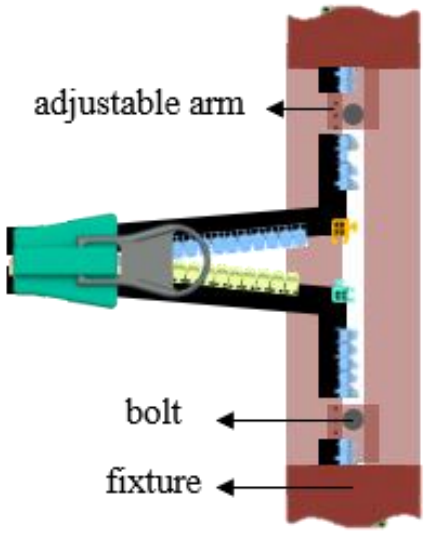

Supplementary Figure 2. The strain adjustment fixture for the tapes when the cross adapter achieves partial interlocking.

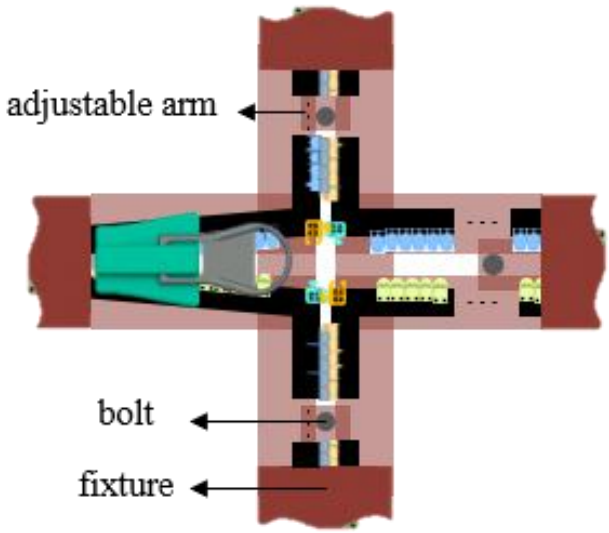

Supplementary Figure 3. The strain adjustment fixture for the tapes when the cross adapter achieves full interlock under symmetric stretching.

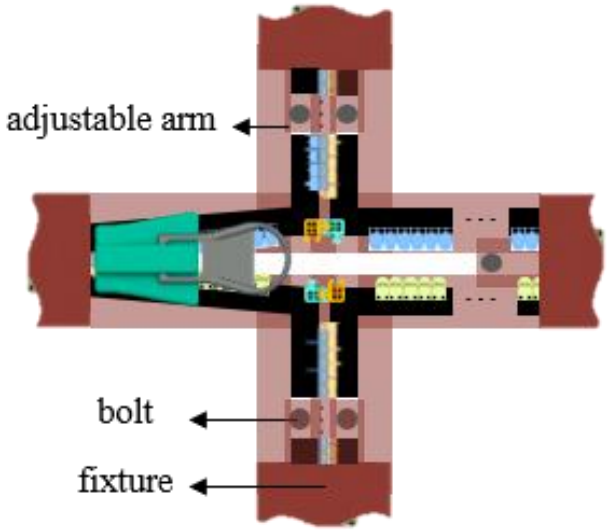

Supplementary Figure 4. The strain adjustment fixture for the tapes when the cross adapter achieves full interlock under asymmetric stretching.

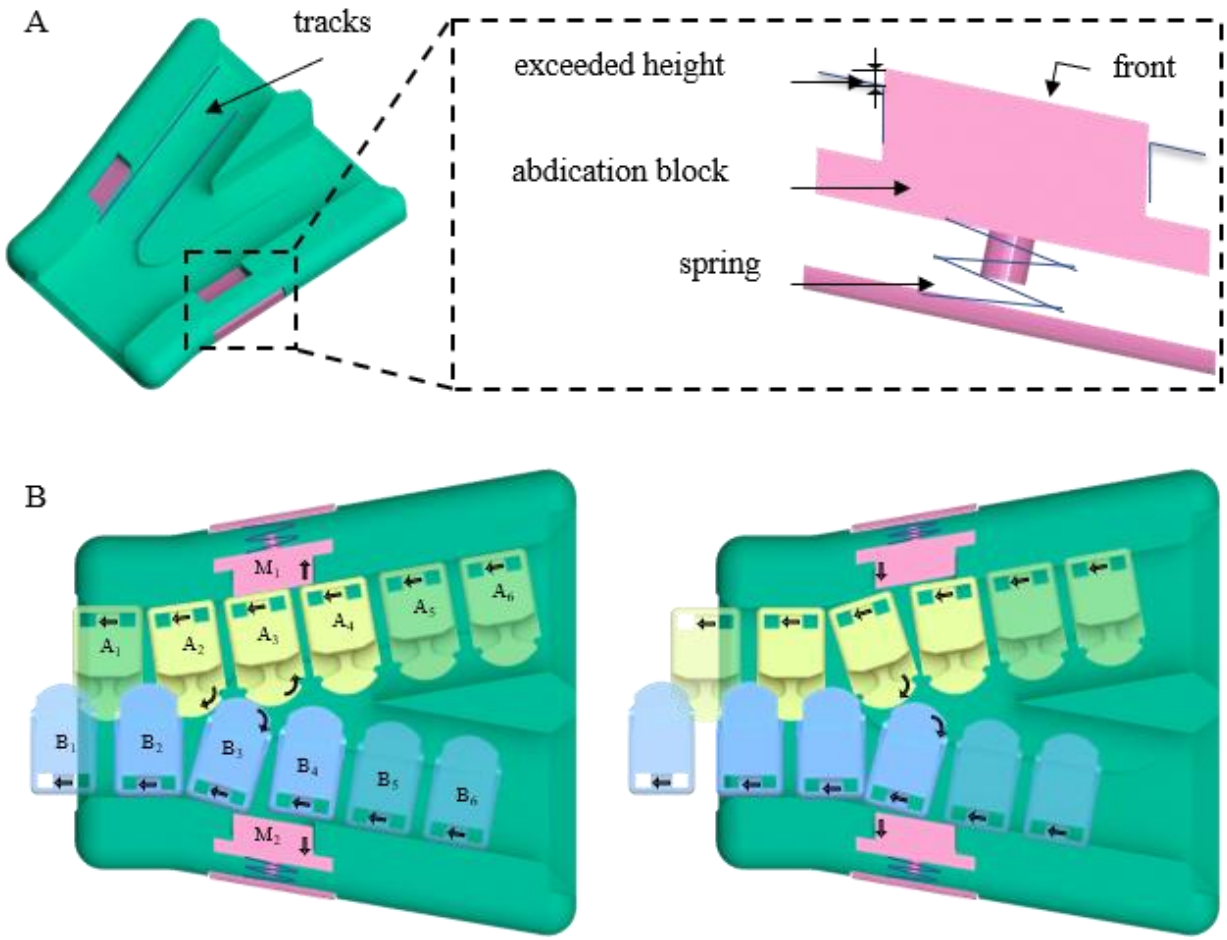

Supplementary Figure 5. Slider structure and tooth motion patterns. (A) Specific structure of the movable abdication block equipped with a spring. During the zipping process, (B) the teeth undergo translation and rotation in the direction indicated by the arrow. The movable abdication blocks, under the action of the spring, repeatedly compress and reset.

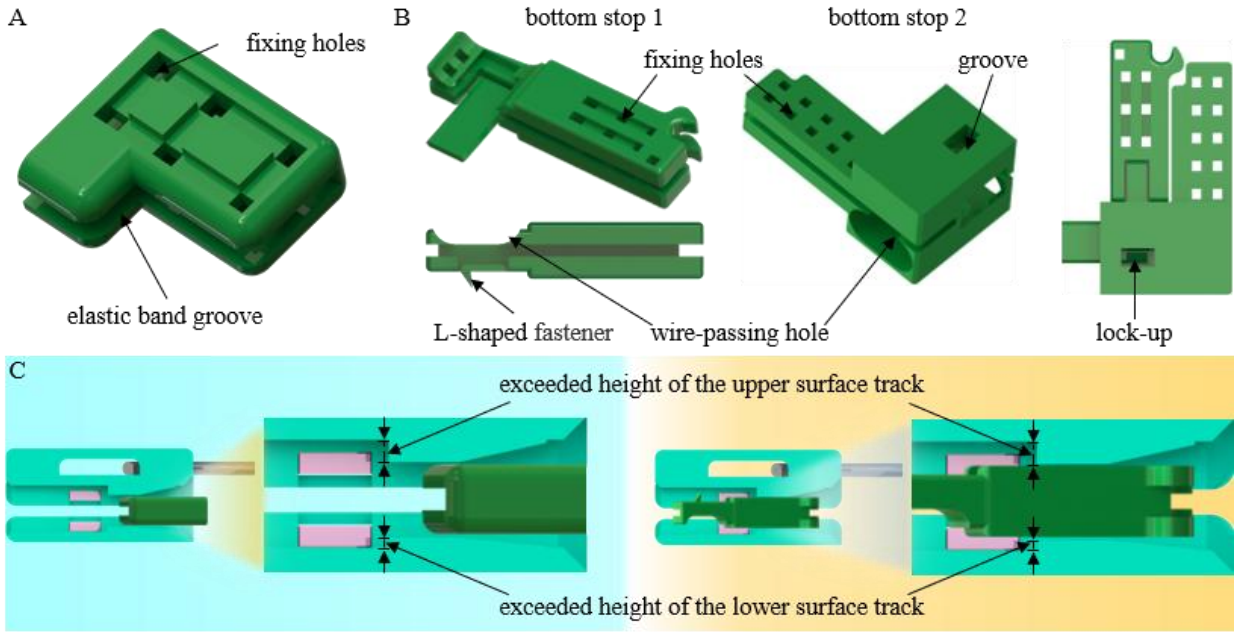

Supplementary Figure 6. The top and bottom stops structures. (A) The specific structure of the top stop; (B) The specific structures of the bottom stops 1 and 2; (C) The spatial positions of the top and bottom stops inside the slider.

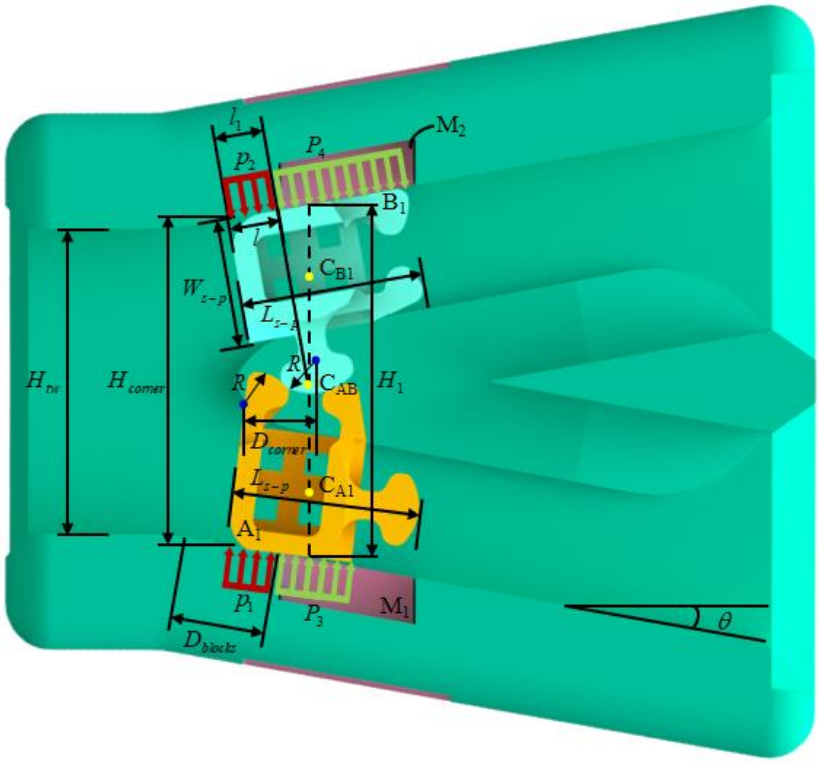

Supplementary Figure 7. Schematic diagram of key areas in the interlocking process of cross adapter.

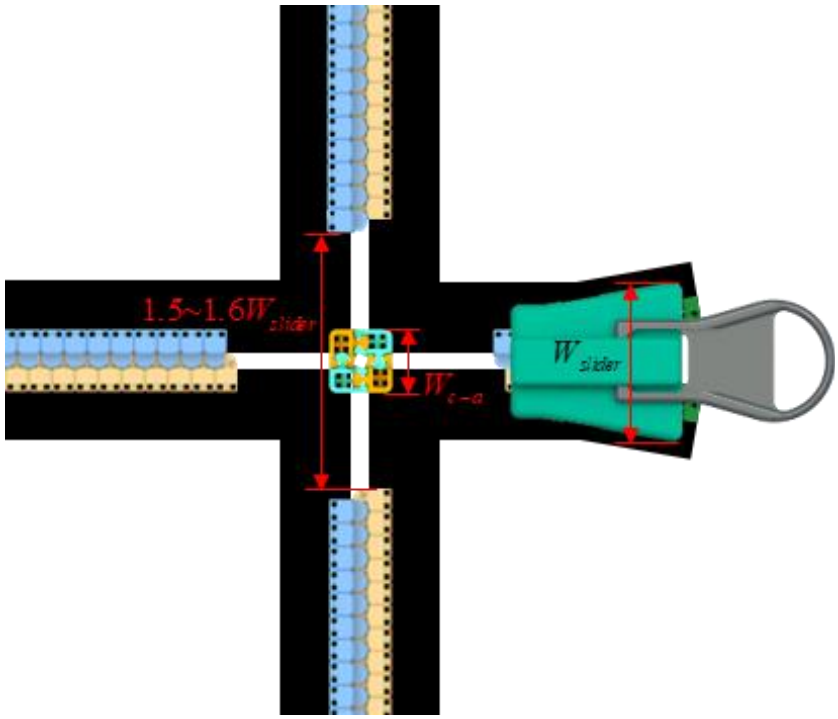

Supplementary Figure 8. Schematic diagram of overlapping area arrangement for crossed stretchable zipper.

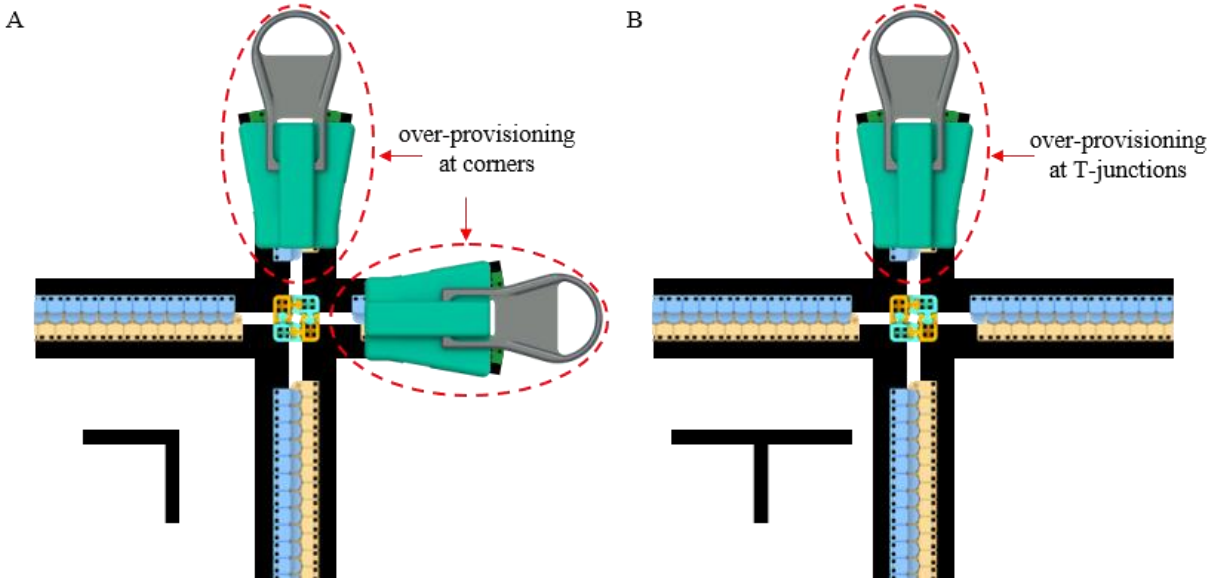

Supplementary Figure 9. Special arrangement of crossed stretchable zippers at different positions. Arrangement of crossed stretchable zippers at (A) corners or (B) T-junctions.

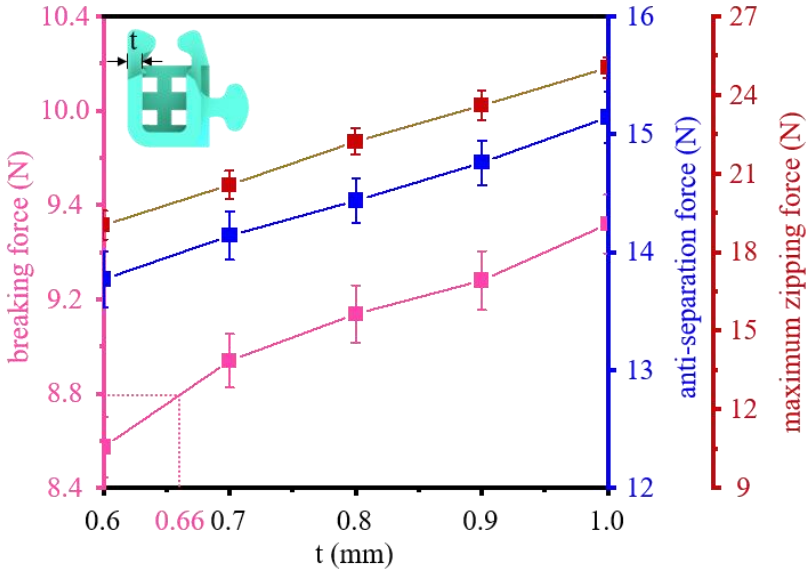

Supplementary Figure 10. Test results for key parameters of the cross adapter across different wall thicknesses.

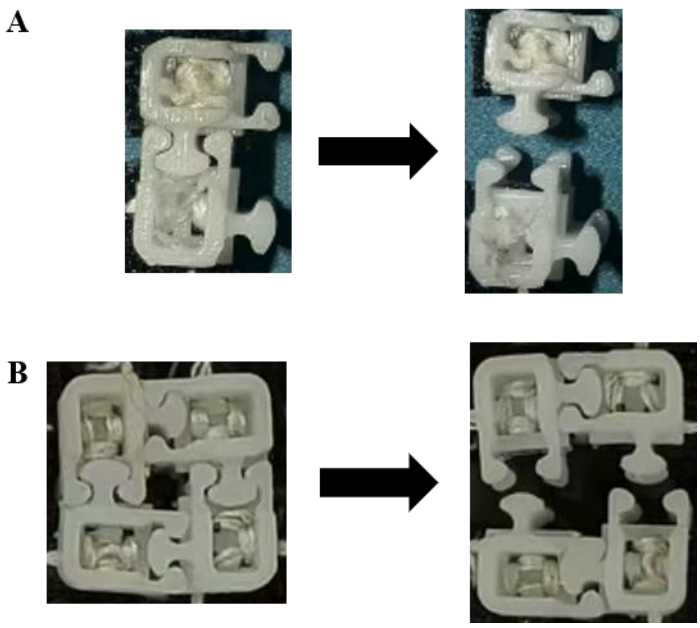

Supplementary Figure 11. The failure modes of cross adapters under scenarios of (A) partial interlock and (B) full interlock.

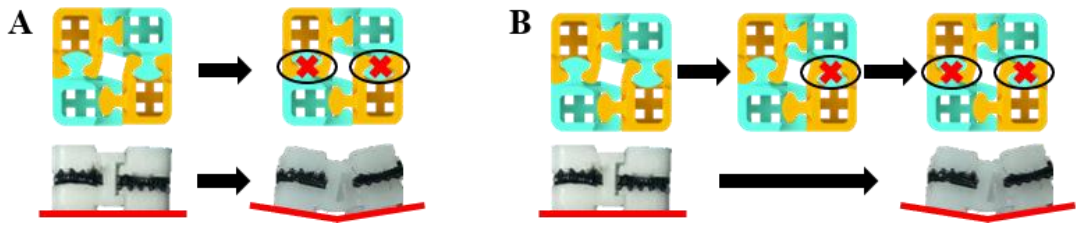

Supplementary Figure 12. The failure sequence of sub-parts after the cross adapter bears a force perpendicular to the interlocking surface in the full interlock scenario. (A) Both groups of sub-parts fail simultaneously under symmetric stretching conditions; (B) The two groups of sub-parts fail successively under asymmetric stretching conditions.

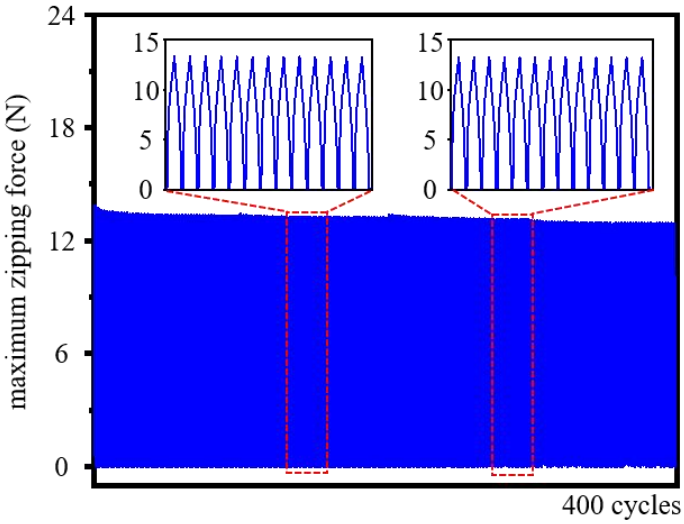

Supplementary Figure 13. Maximum zipping force drift of crossed stretchable zipper after 400 cycles.

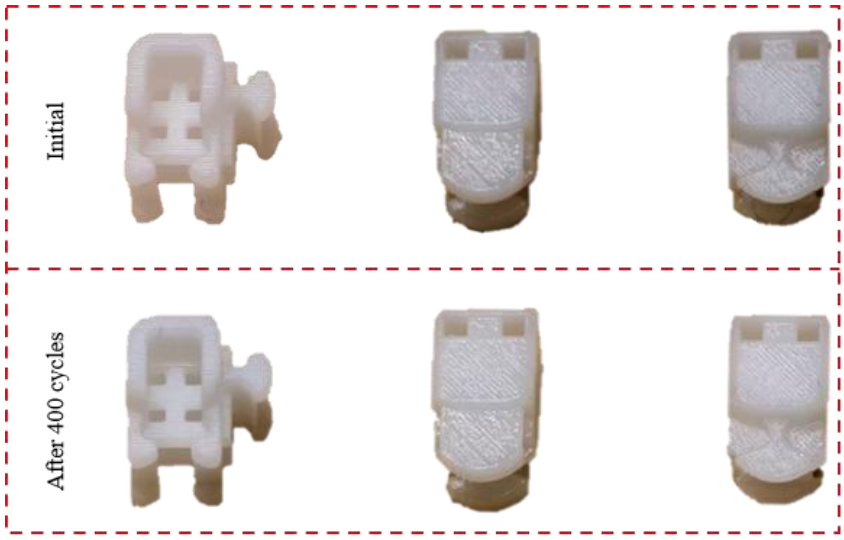

Supplementary Figure 14. Wear of teeth and cross adapters before and after the zipper zipping/unzipping cycles.

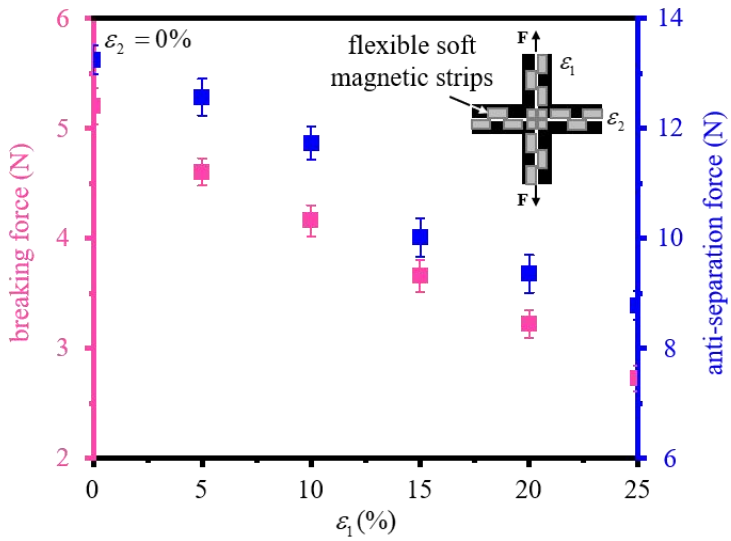

Supplementary Figure 15. Breaking force and anti-separation force of magnetic closure cross zippers under different strain conditions.

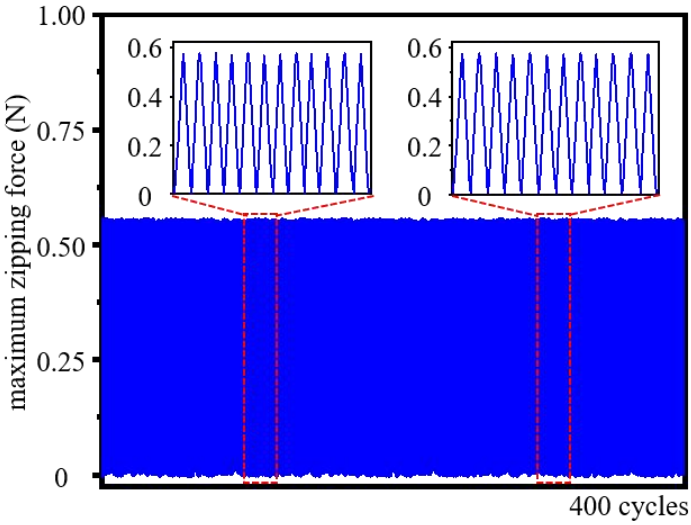

Supplementary Figure 16. Maximum zipping force drift of magnetic closure cross zipper after 400 cycles.

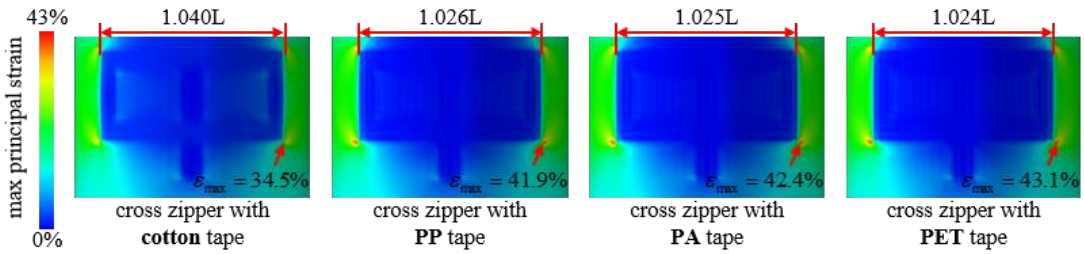

Supplementary Figure 17. Strain distribution in the zipper-covered area of bodysuits with crossed zippers based on different tapes during static respiration.

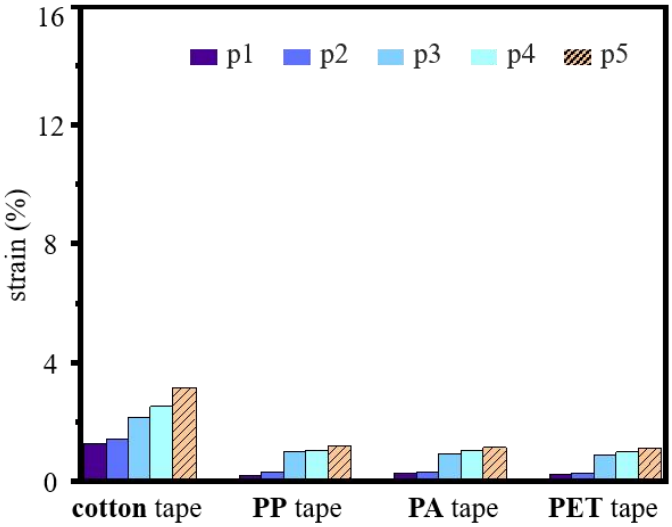

Supplementary Figure 18. The strain of the bodysuit in five key areas covered by the cross zipper with different tapes.

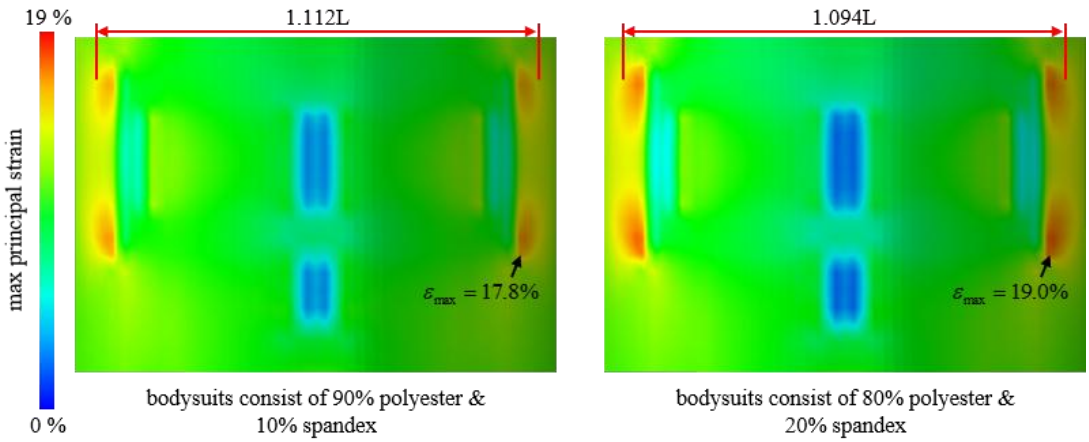

Supplementary Figure 19. Strain distribution in the zipper-covered area of different bodysuits during static respiration.

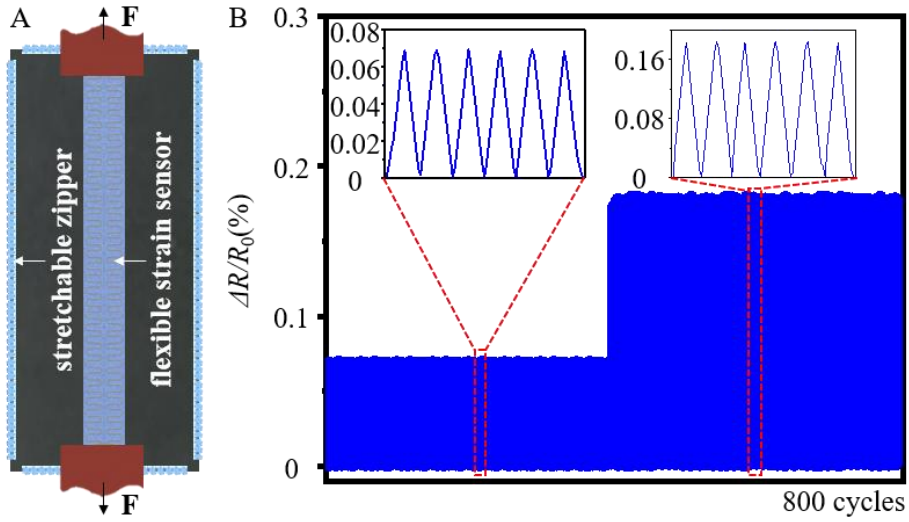

Supplementary Figure 20. Signal stability of flexible strain sensors under different stretching conditions.